Available online at www.sciencedirect.com
SCIENCE DIRECT®

Journal of the European Ceramic Society 24 (2004) 171–178

www.elsevier.com/locate/jeurceramsoc

Boron carbide and nitride as reactants for in situ synthesis of boride-containing ceramic composites

G.J. Zhang[a,*], M. Ando[a], J.F. Yang[b], T. Ohji[b], S. Kanzaki[b]

[a]*Synergy Ceramics Laboratory, Fine Ceramics Research Association (FCRA), Nagoya, Aichi 463-8687, Japan*
[b]*Synergy Materials Research Center, National Institute of Advanced Industrial Science and Technology (AIST), Nagoya, Aichi 463-8687, Japan*

Abstract

Using boron carbide (B_4C) and boron nitride (here refers to hexagonal BN) as reactants, a series of boride-containing ceramic composites, mainly in the present work zirconium diboride-containing composites including zirconium diboride–zirconium carbide (ZrB_2–ZrC), zirconium diboride–zirconium nitride (ZrB_2–ZrN), zirconium diboride–silicon carbide (ZrB_2–SiC) and zirconium diboride–aluminum nitride (ZrB_2–AlN) were prepared by in situ reactive hot pressing. The features and the development mechanisms of the composite microstructures were characterized and modeled. The obtained zirconium diboride-containing composites demonstrated high bending strength. In addition, some general problems such as transformation between B_4C and BN and thermodynamics of using B_4C and BN as reactants were also briefly discussed.

Keywords: B_4C; BN; Ceramic composites; Reaction synthesis; TiB_2; ZrB_2

1. Introduction

Boride ceramics are important materials, include (1) B_4C with low density and extreme tribological properties used as wear-resistant materials or armor, and nuclear characteristics used as neutron absorber. (2) BN with high hardness in its cubic type (c-BN) used as cutting tool material or excellent thermal shock resistant and lubricant characteristics in its hexagonal type (h-BN) used as high temperature refractory or lubricating material. (3) TiB_2 and ZrB_2 with high hardness, corrosion resistance to chemicals or molten metal and electrical conductivity used as cutting tools and electrodes. In addition, they also demonstrate good ballistic performance. Other borides, such as superconductor MgB_2, has attracted much attention from researchers very recently.

Boride-containing ceramic composites show better properties over monoliths through careful design.[1–12] For example, the toughness of SiC ceramics can be improved by adding TiB_2 or ZrB_2 particles through particulate toughening mechanism and the oxidation resistance of TiB_2 or ZrB_2 ceramics can be enhanced by adding SiC particles. The mechanical properties of TiB_2 can also be improved by the addition of ZrO_2 through transformation toughening mechanism.[2]

Boride-containing composites can either be produced by sintering of the mixed powders of component phases or synthesized based on some reaction sintering processes. ZrB_2–ZrC composites were produced by the directed reaction of molten Zr to the B_4C preform[13] and Ti–B–C composites were prepared by the transient plastic phase processing using Ti and B_4C as reactants.[14,15] AlN–TiB_2 composite was synthesized from the Al–Ti–BN reaction system[16] and SiC–TiB_2 composite was prepared by the reaction of Si, Ti and B_4C.[17] In this article we will discuss three items concerning the reaction synthesis of boride-containing composites using B_4C and BN as reactants: thermodynamic analysis, transformation between B_4C and BN, and the microstructural features of the obtained composites with ZrB_2 composites as examples.

2. Thermodynamic consideration

2.1. Transformation between B_4C and BN

The thermodynamic calculations of the phase equilibria in the B–C–N–O system have been well performed.[18] It is pointed out that B_4C is only stable at

* Corresponding author.
E-mail address: zh77@yahoo.com (G.J. Zhang).

0955-2219/$ - see front matter © 2003 Elsevier Ltd. All rights reserved.
doi:10.1016/S0955-2219(03)00607-1

high temperatures and BN is stable over a large temperature range in nitrogen atmosphere. Manufacture of B_4C powder is in general conducted in argon atmosphere.[19] The nitridation reaction of B_4C in N_2 atmosphere is:

$$B_4C(s) + 2N_2(g) \rightarrow 4BN(s) + C(s) \quad (1)$$

According to the thermodynamic data,[20] we can calculate out the enthalpy of reaction (1) at standard condition to be $\Delta H^\circ_{298} = -940.98$ kJ, indicating reaction (1) to be an exothermic reaction. The free enthalpy $\Delta G^\circ(T)$ function in the temperature range of 298∼2200 K is as follows:

$$\Delta G^\circ_T = \Delta H^\circ_{298} - T\Delta S^\circ = -940980 + 341.215T \quad (J)$$

We can see that $\Delta G^\circ{}_T$ is a large negative value in the experiment temperature range demonstrating the thermodynamic possibility of the reaction ($T = 2485$ °C when $\Delta G^\circ{}_T = 0$). The equilibrium N_2 pressure P_{N2} for reaction (1) at different temperature can be calculated out from:

$$\Delta G^\circ_T = -RTLnKp = -RTLnP^{-2}_{N2} = 2RTLnP_{N2}$$

For example, $P_{N2} = 1.69\times10^{-3}$ Pa at $T = 1200$ °C, $P_{N2} = 1.12$ Pa at $T = 1500$ °C and $P_{N2} = 1.26\times10^{3}$ Pa at $T = 2000$ °C. It can be seen that B_4C changes to BN very easily in N_2 atmosphere. For reaction bonded silicon nitride (RBSN), B_4C has been utilized to generate volume expansion during its nitridation process to fill the residual pores in RBSN for achieving dense ceramic body.[21,22]

2.2. In situ formation of BN from reactions between B_4C and solid state nitrogen-bearing reactants

As mentioned above, B_4C can change to BN in N_2 atmosphere. Moreover, it can react with solid state nitrogen-bearing components to form BN in Ar or N_2 atmosphere. For example, SiC–BN composites can be synthesized through the following reaction:[23,24]

$$Si_3N_4 + B_4C + 2C = 3SiC + 4BN \quad (2)$$

The free enthalpy $\Delta G^\circ(T)$ function in the temperature range of 298∼2200 K is as follows:

$$\Delta G^\circ_T = \Delta H^\circ_{298} - T\Delta S^\circ = -415888 + 43.846T \quad (J)$$

The reaction is exothermic and thermodynamically possible. However, due to the reaction process being closely related to the decomposition process of Si_3N_4, Ar atmosphere is beneficial to the completion of the reaction.[25] The in situ formed h-BN flakes are homogeneously and isotropically distributed in the SiC matrix.[26] By the way, a similar reaction[27] do not exist for producing the relative TiC–BN composite because that the actual reaction will be $4TiN + B_4C + C = 2TiC + 2TiB_2 + 2N_2$.

2.3. Reactions containing B_4C and BN as reactants

Many boride-containing ceramic composites can be synthesized by using B_4C and BN as reactants. Some of these reactions are listed in Table 1. It can be seen that except for reaction (11), the reactions are highly exothermic and satisfy the thermodynamic conditions for self-sustaining combustion process ($T_{ad} \geqslant 1800$ K and $\Delta H^\circ_{298}/C_{p298} > 2000$ K).[28] It means that these composites can be produced by self-propagating high-temperature synthesis (SHS) based on thermodynamic consideration. On the other hand, if reactive hot pressing (RHP) is being used to prepare dense blocks of these composites, heating rate should be controlled to prevent the reactions from becoming self-sustaining. In general, a heating rate of slower than 10 °C/min is selectable.

3. Experimental procedure

The starting powders used for preparing SiC–BN composite were Si_3N_4 (E-10 grade, particle size 0.5 μm, Ube Industries, Yamaguchi, Japan), B_4C (F1 grade,

Table 1
Reactions and thermodynamic data

Reaction	Enthalpy ΔH°_{298} (J)	Free enthalpy ΔG° at 1500 K (J)	$\Delta H^\circ_{298}/C_{p298}$ (K)	Adiabatic temperature T_{ad} (K)
(3) $3Ti + B_4C = 2TiB_2 + TiC$	−680 402	−613 665	5560	3193 (TiB_2 mp)
(4) $3Zr + B_4C = 2ZrB_2 + ZrC$	−779 144	−718 609	5798	3323 (ZrB_2 mp)
(5) $3Ti + 2BN = TiB_2 + 2TiN$	−452 961	−407 289	3824	2650
(6) $3Zr + 2BN = ZrB_2 + 2ZrN$	−551 284	−511 498	4269	3138
(7) $2Ti + Si + B_4C = 2TiB_2 + SiC$	−569 526	−509 429	4935	2696
(8) $2Zr + Si + B_4C = 2ZrB_2 + SiC$	−655 716	−596 171	5317	3094
(9) $Ti + 2Al + 2BN = TiB_2 + 2AlN$	−413 631	−321 929	3959	2268
(10) $Zr + 2Al + 2BN = ZrB_2 + 2AlN$	−456 726	−365 300	4212	2464
(11) $2Ti + 3Si + 4BN = 2TiB_2 + Si_3N_4$	−300 078	−279 866	1595	1320
(12) $4.5Ti + B_4C + BN = 2.5TiB_2 + 2TiC_{0.5}N_{0.5}$	−906 883	−817 310	4994	3067
(13) $4Al + 3TiO_2 + 2BN = 2Al_2O_3 + TiB_2 + 2TiN$	−988 179	−796 361	3574	2303 (Al_2O_3 mp)
(14) $4Al + 3TiO_2 + B_4C = 2Al_2O_3 + 2TiB_2 + TiC$	−121 562	−1 002 737	4335	2423

mean particle size 1 μm, Denki Kagaku Kogyo, Ltd., Tokyo, Japan) and C (2600# grade, particle size 13 nm, Mitsubishi Chemical, Tokyo, Japan) and those used for preparing ZrB_2-containing composites were Zr (particle size <50 μm, High Purity Chemicals Laboratory, Saitama, Japan), Si (particle size <50 μm, High Purity Chemicals Laboratory, Saitama, Japan), Al (mean particle size 3 μm, High Purity Chemicals Laboratory, Saitama, Japan), B_4C (F1 grade) and BN (SP-2 grade, mean particle size 4 μm, Denki Kagaku Kogyo Co.Ltd., Tokyo, Japan).

The morphologies of the starting powders for preparing ZrB_2-containing composites are shown in Fig. 1. For Zr and Si powders, although most of the particles are smaller than 10 and 5 μm, respectively, there are some large particles with about 50 μm in particle size. The mean particle size of B_4C powder is small, but the particle size distribution is very broad and there are many large particles of about 5 μm. For BN powder, most of the particles are finer than 1 μm except for some large flakes with a diameter of less than 10 μm. Obviously, the particle sizes of the non-metallic reactants are smaller than those of the metallic reactants. The morphologies of the starting powders for preparing SiC–BN composite have ever been illustrated in a previous paper.[24]

The stoichiometric powders according to reactions (2), (4), (6), (8) and (10), respectively, were mixed in ethanol with $ZrO_2(Y_2O_3)$ balls for 24 h in a plastic bottle and then dried. The composites were produced by reactive hot pressing in a graphite die with BN coating at 2000 °C for SiC–BN composite and 1900 °C for ZrB_2-containing composites, respectively, under 30 MPa for 60 min in an Ar atmosphere. The dried mixed powders were placed into a cold graphite die and loaded to 20 MPa before increasing the temperature. Below 1100 °C the furnace was kept at a vacuum of about 10^{-4} torr. Then Ar gas was inlet into the chamber up to 1.3 atm. Since the reactions are exothermic with large enthalpies of reaction, slow heating rate (10 °C/min)

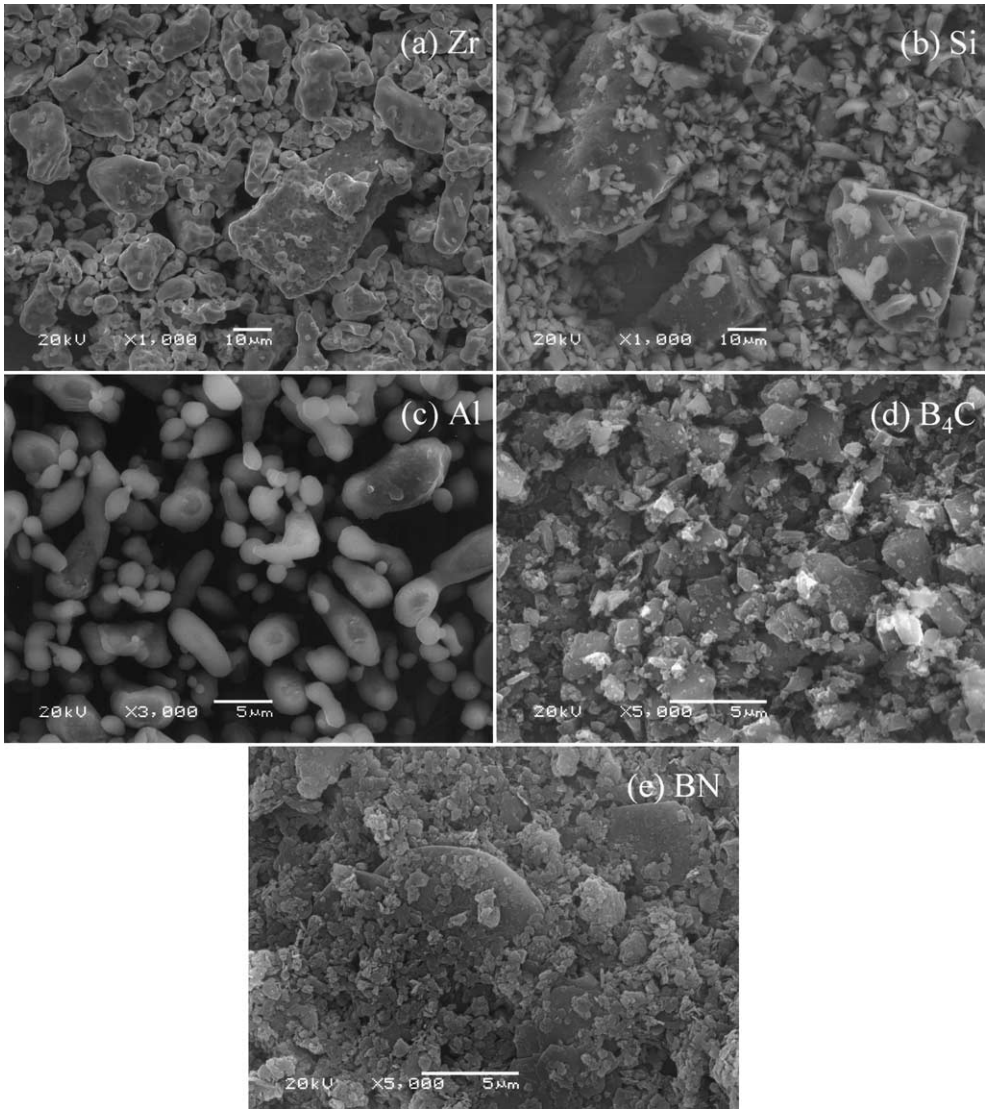

Fig. 1. Morphologies of the starting powders for preparing ZrB_2-containing composites.

Table 2
Calculated phase compositions, phase compositions determined by XRD, measured relative densities and strength of the obtained composites by RHP

Composite	Calculated phase composition (vol.%)	Phase composition determined by XRD	Relative density (TD%)	Bending strength (MPa)
SiC–BN	46.29:53.71	β-SiC, t-BN	70.6	56.4±7.2
ZrB_2–ZrC	70.73:29.27	ZrB_2, ZrC	98.4	452.3±45.1
ZrB_2–ZrN	38.03:61.97	ZrB_2, ZrN, a little ZrO_2	100.8	581.7±34.9
ZrB_2–SiC	74.85:25.15	ZrB_2, β-SiC	96.9	547.8±33.5
ZrB_2–AlN	42.42:57.58	ZrB_2, AlN	99.1	562.7±39.9

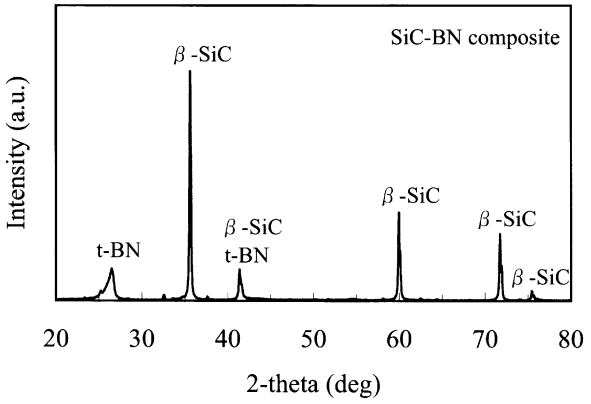

Fig. 2. XRD pattern (CuK_α radiation) of the obtained SiC–BN composite.

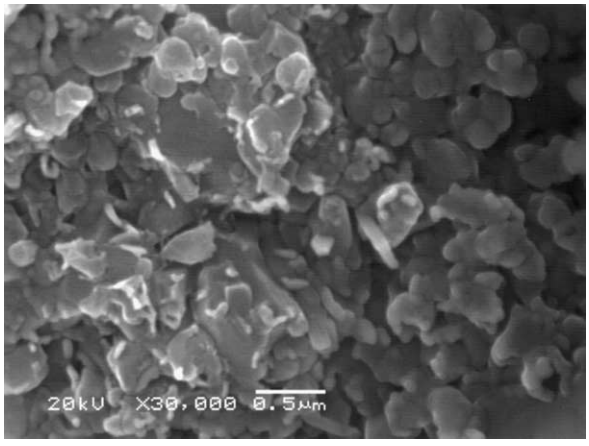

Fig. 3. Microstructure of the SiC–BN composite observed by SEM.

was adopted for preventing the reaction from becoming self-sustaining. For preventing the molten aluminum or silicon from moving out of the die at high temperatures, the pressure was started at 1550 °C and gradually increased to 30 MPa before the temperature reaching 1900 °C.

The obtained products had diameters of 25 mm and thicknesses of 6 mm. After removing the surface layers by gringing, phase composition was determined by X-ray diffraction (XRD) using CuK_α radiation. The density was tested by water displacement method. Density values of 3.22 g/cm^3 for SiC, 2.27 g/cm^3 for BN, 6.09 g/cm^3 for ZrB_2, 6.73 g/cm^3 for ZrC, 6.97 g/cm^3 for ZrN and 3.26 g/cm^3 for AlN were used in the calculation of the theoretical densities of the obtained composites. Specimens for strength measurement were cut from the products and then ground with diamond wheel (600 grit size) along the longitudinal direction of the specimens. The four edges of specimens were beveled using 1000 grit diamond wheel. The three-point bending strength was measured on bars with dimensions of 2.5×3×20 mm. The span was 16 mm and the crosshead speed was 0.5 mm/min. The strength data were an average of three measurements. The fracture surfaces of the composites were observed by a scanning electron microscopy (SEM, JEOL JSM-5600 at 20 kV) or a field emission scanning electron microscopy (FE-SEM, JEOL JSM-6330F at 15 kV). The crystalline grains were determined by energy dispersive X-ray spectrometry (EDX).

4. Results and discussion

4.1. Results

The calculated phase compositions in volume percentage, the phase compositions determined by XRD, the measured relative densities and bending strength of the obtained composites are listed in Table 2. The obtained SiC–BN composite showed low strength because of the low relative density. On the other hand, however, the ZrB_2-containing composites exhibited high strength.

4.2. In situ formation of BN

The relative densities of the obtained SiC–BN composite are 70.6%TD. From the previous results, dense composites can be manufactured with the addition of liquid phase-forming sintering aids such as Al_2O_3–Y_2O_3.[29] From the XRD pattern of the composite shown in Fig. 2 it can be seen that the phase composition is in accordance with the product of the reaction (2). Fig. 3 shows the microstructure of the composite. We can find that the obtained composite demonstrates very fine and

homogeneous microstructure. The in situ formed BN and SiC particles are in quasi-spherical shape. The reason for the quasi-spherical shape of BN is considered to be the nonexistence of liquid phase forming sintering additives. Our previous work has pointed out that liquid phase forming sintering additives, such as Al_2O_3–Y_2O_3, can enhance the growth of BN flakes by recrystallization of the formed turbostratic BN (t-BN).[29]

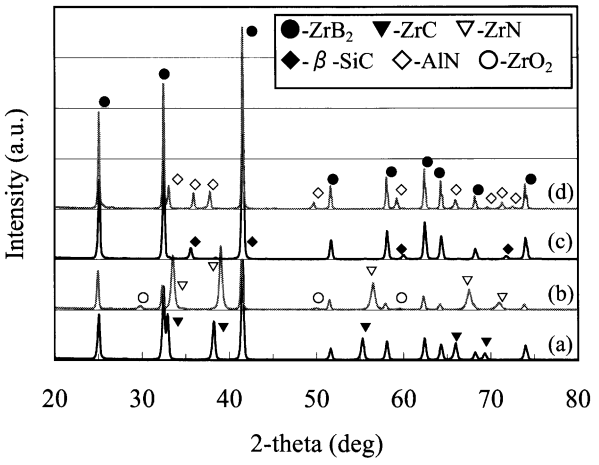

Fig. 4. XRD patterns (CuK_α radiation) of the obtained ZrB_2-containing composites prepared by RHP: (a) ZrB_2–ZrC composite; (b) ZrB_2–ZrN composite; (c) ZrB_2–SiC composite; (d) ZrB_2–AlN composite.

4.3. ZrB_2-containing composites

Among these four ZrB_2-containing composites, the ZrB_2–SiC composite showed the lowest relative density and the ZrB_2–ZrN composite showed the highest relative density. Owing to the difference between the calculated and the actual phase composition, there should be some error in relative density such as the data of over 100% for the ZrB_2–ZrN composite. Fig. 4 shows the XRD patterns of the composites prepared by RHP. Except that there exists a small amount of ZrO_2 phase in ZrB_2–ZrN composite, the main phase compositions in the obtained products are in accordance with the correspond reactions. The appearance of ZrO_2 in ZrB_2–ZrN composite is suggested to be from the small amount of B_2O_3 existed in BN starting powder.

The microstructures of the composites are demonstrated in Fig. 5. It can be found that the microstructures are very different among these composites although the same Zr powder was used. In ZrB_2–ZrC composite, there are large ZrC agglomerates surrounded by fine ZrB_2 and ZrC particles. However, the microstructure of the ZrB_2–ZrN composite is very fine

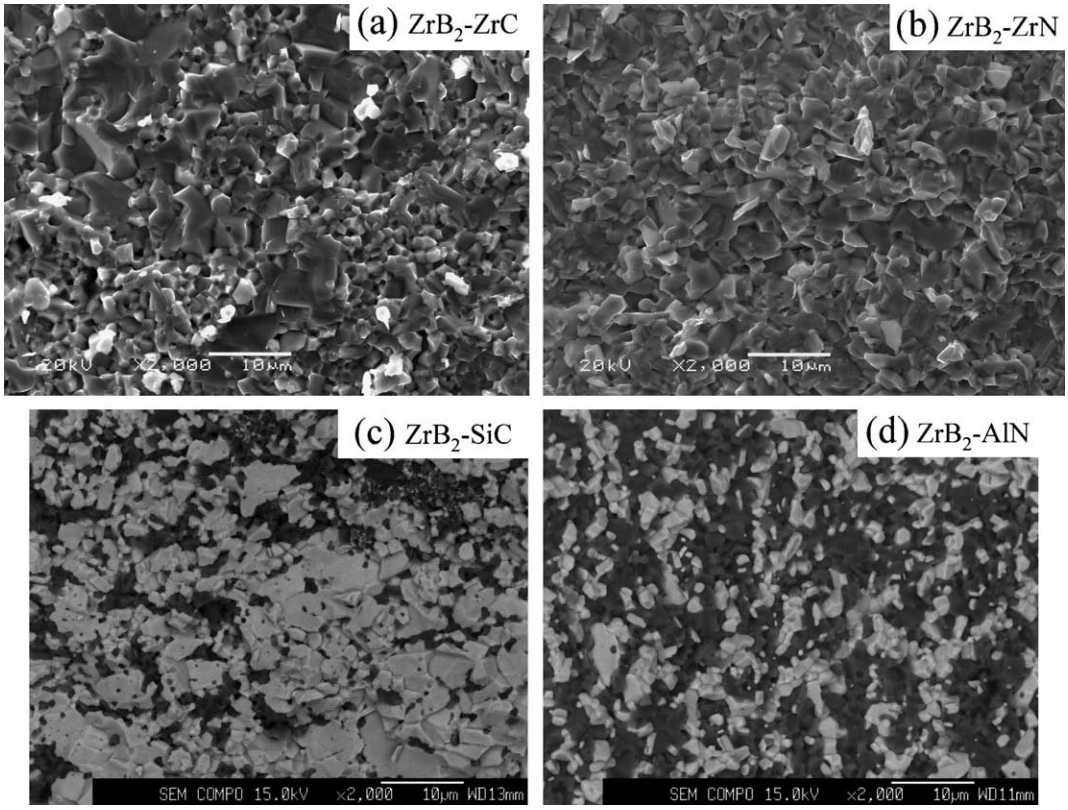

Fig. 5. Microstructures of the obtained ZrB_2–containing composites observed by SEM or FE-SEM: (a) ZrB_2–ZrC composite showing the large ZrC agglomerates; (b) ZrB_2–ZrN composite showing the fine and homogeneous microstructure; (c) ZrB_2–SiC composite indicating the existence of large ZrB_2 agglomerates (white) and small SiC particles (gray); (d) ZrB_2–AlN composite demonstrating the fine and homogeneous microstructure (white is ZrB_2 and gray is AlN).

and homogeneous although we could not distinguish the grains of ZrB_2 and ZrN. In ZrB_2–SiC composite, there are many large ZrB_2 agglomerates (the white phase is ZrB_2 and the gray one is SiC) with the particle size level of Zr starting powder. On the other hand, however, the microstructure of ZrB_2–AlN is very fine and homogeneous (the white phase is ZrB_2 and the gray one is AlN).

There are many factors affecting the microstructures of the in situ reaction synthesized composites, such as particle size of starting powders, heating and applied load programs, atmosphere, reaction mechanisms including formation of transient phases, reaction kinetics including diffusion coefficients of the component atoms or ions, and phase composition of the final obtained composite. In the present case, the same Zr starting powder, the same Ar atmosphere and totally same heating and applied load programs were used. Thus, different reaction mechanisms and kinetics should have resulted in the different microstructures of the composites. In Zr–B_4C system for preparing ZrB_2–ZrC composite, due to the diffusion coefficient of carbon being much faster than that of boron in zirconium, only carbon can reach the center of the large Zr particles and results in the micrograph with large ZrC agglomerates surrounded by fine ZrB_2 and ZrC particles. In Zr–BN system for preparing ZrB_2–ZrN composite, although we could not find available data for the diffusion coefficient of B and N in Zr, we infer that the diffusion coefficient of N is smaller than that of C but close to that of B. Accordingly, homogeneous microstructure can be obtained by the inter-constraint of grain growth of the formed two phases. Abnormal grain growth of ZrB_2 and ZrN can also be effectively restrained.[30]

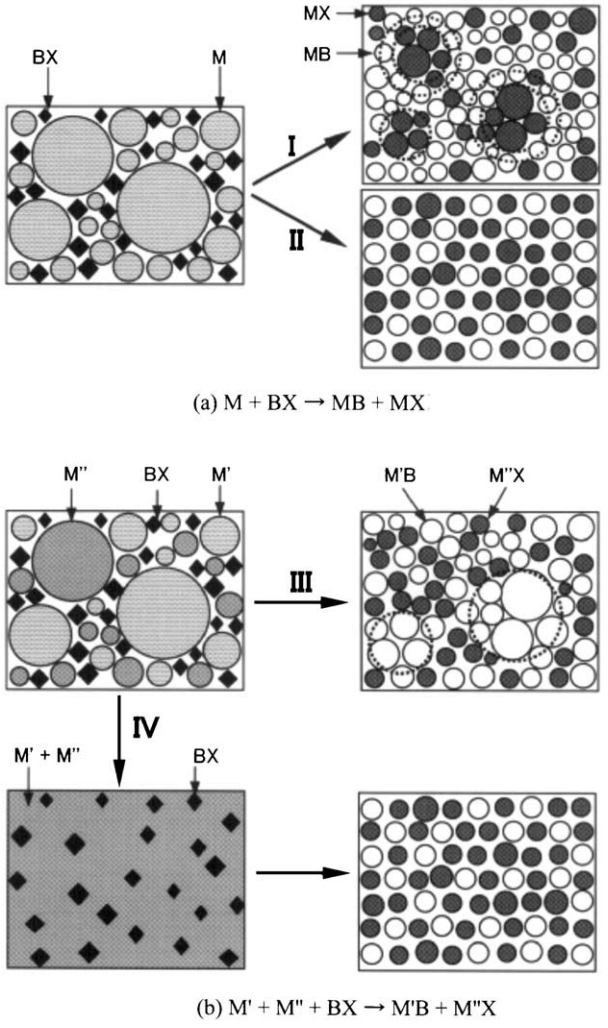

Fig. 6. Schematic illustration of the microstructural features of the obtained ZrB_2–containing composites. ZrB_2–ZrC and ZrB_2–ZrN composites correspond to the case I and II, respectively. ZrB_2–SiC and ZrB_2–AlN composites correspond to the case III and IV, respectively. The dotted circles in case I represent the size of Zr starting powder (outside one) and the agglomerate size of ZrC (inside one), respectively. The dotted circles in case III represent the size of Zr starting powder, also the size of ZrB_2 agglomerates.

In Zr–Si–B_4C system for preparing ZrB_2–SiC composite, due to the B and C from B_4C diffuse to Zr and Si, respectively, the formed microstructure demonstrates the features of the particles of the starting reactants. On the other hand, however, due to the melting point of Si being as low as 1414 °C, the formed SiC agglomerates are small. In addition, the solubility of Si in Zr or Zr in Si is very small,[31] thus the re-distribution of Zr and Si by solution process is not remarkable although some SiC particles can be found in the large ZrB_2 agglomerates [see Fig. 5(c)]. Moreover, it is suggested that there is not enough time for the diffusion of Si into Zr to form transient phase of zirconium silicides during the RHP process.

In Zr–Al–BN system for preparing ZrB_2–AlN composite, Al will melt at temperature as low as 660 °C and the maximum solubilities of Al in α-Zr and β-Zr are as large as 11.5 and 26 at.%, respectively.[31] Accordingly, re-distribution process of Zr and Al is remarkable in this system, thus fine and homogeneous microstructure can be obtained. Fig. 6 shows the schematic illustration of the microstructural features of the obtained composites. ZrB_2–ZrC and ZrB_2–ZrN composites correspond to the case I and II, respectively, in Fig. 6(a). Actually, it can be realized that ZrB_2–ZrC composite with fine and homogeneous microstructure could be synthesized by using Zr powder with fine particle size. ZrB_2–SiC and ZrB_2–AlN composites correspond to the case III and IV, respectively, in Fig. 6(b). It can be noticed that the agglomerate size in case III should be larger than that in case I. The same as for the ZrB_2–ZrC composite, fine and homogeneous microstructure in ZrB_2–SiC composite could be obtained by using fine Zr starting powder. It should be pointed out that the actual reaction processes and microstructural development mechanisms may be much complicated than those illustrated here, for example, in case IV the M′ + M″ should include either solution or intermetallics. Moreover, in all cases

transient phases should exist and the appearance of those phases are dependent on the heating program.

5. Summary

Thermodynamics, transformation between B_4C and BN, and the microstructural features of the boride-containing composites with ZrB_2 composites as examples using B_4C and BN as reactants are discussed. These in situ reactions are highly exothermic and satisfy the conditions for self-sustaining combustion process, thus, if RHP is being used to prepare dense blocks of these composites, heating rate should be controlled to prevent the reactions from becoming self-sustaining. Although the same Zr powder with large particle size is used, the obtained composites ZrB_2–ZrC, ZrB_2–ZrN, ZrB_2–SiC and ZrB_2–AlN by RHP show very different microstructures. An explanation and a schematic microstructure development mechanism based on the reaction and diffusion process were proposed. ZrB_2–ZrC and ZrB_2–SiC composites with fine and homogeneous microstructures should be produced by using fine Zr starting powder. A similar mechanism might also exist in TiB_2-containing composites synthesized by using Ti, Si, Al, B_4C and BN as reactants.

Acknowledgements

This work has been supported by AIST, METI, Japan, as part of the Synergy Ceramics Project. Part of the work has been supported by NEDO. The authors are members of the Joint Research Consortium of Synergy Ceramics. The authors are grateful to Ms. Ying Hu at Synergy Materials Research Center, AIST for XRD and FE-SEM analysis.

References

1. Telle, R., Boride and carbide ceramics. In *Materials Science and Technology*, ed. R. W. Cahn, P. Haasen and E. J. Kramer. Verlag Chemie, Weinheim, Germany, 1993, pp. 175–266.
2. Watanabe, T. and Shobu, K., Mechanical properties of hot pressed TiB_2–ZrO_2 composites. *J. Am. Ceram. Soc.*, 1985, **68**(2), C–34–C-36.
3. Telle, R. and Petzow, Z., Strengthening and toughening of boride and carbide hard material composites. *Mater. Sci. Eng.*, 1988, **A105/106**, 97–104.
4. Watanabe, T., Yamamoto, H., Shobu, K. and Sakamoto, T., Factors affecting the porosity and bending strength of Ti(CN)–TiB_2 materials. *J. Am. Ceram. Soc.*, 1988, **71**(4), C–202–C-204.
5. Zhang, G. J., Jin, Z. Z. and Yue, X. M., TiN–TiB_2 composites prepared by reactive hot pressing and effects of Ni addition. *J. Am. Ceram. Soc.*, 1995, **78**(10), 2831–2833.
6. Zhang, G. J., Yue, X. M., Jin, Z. Z. and Dai, J. Y., In-situ synthesized TiB_2 toughened SiC. *J. Eur. Ceram. Soc.*, 1996, **16**, 409–412.
7. Bellosi, A. and Monteverde, F., Microstructure and properties of titanium nitride and titanium diboride-based composites. *Key Eng. Mater.*, 2000, **175-176**, 139–148.
8. Yorihiro, M. and Dean Batha, H., Densification and wear resistance of TaN–ZrB_2–ZrN and TaN–ZrB_2–WC compositions. *Am. Ceram. Soc. Bull.*, 1981, **60**(8), 818–824.
9. Takahash, K. and Jimbou, R., Effect of uniformity on the electrical resistivity of SiC–ZrB_2 ceramic composites. *J. Am. Ceram. Soc.*, 1987, **70**(12), C–369–C-373.
10. Tripp, W. C., Davis, H. H. and Graham, H. C., Effect of an SiC addition on the oxidation of ZrB_2. *Am. Ceram. Soc. Bull.*, 1973, **52**(8), 612–616.
11. Zhang, G. J., Deng, Z. Y., Kondo, N., Yang, J. F. and Ohji, T., Reactive hot pressing of ZrB_2–SiC composites. *J. Am. Ceram. Soc.*, 2000, **83**(9), 2330–2332.
12. de Mestral, F. and Thevenot, F., Ceramic composites: TiB_2–TiC–SiC, part I properties and microstructures in the ternary system. *J. Mater. Sci.*, 1991, **26**, 5547–5560.
13. Johnson, W. B., Nagelberg, A. S. and Breval, E., Kinetics of formation of a platelet-reinforced ceramic composite prepared by the directed reaction of zirconium with boron carbide. *J. Am. Ceram. Soc.*, 1991, **74**(9), 2093–2101.
14. Barsoum, M. W. and Houng, B., Transient plastic phase processing of titanium–boron–carbon composites. *J. Am. Ceram. Soc.*, 1993, **76**(6), 1445–1451.
15. Brodkin, D., Kalidindi, S. R., Barsoum, M. W. and Zavaliangos, A., Microstructural evolution during transient plastic phase processing of titanium carbide–titanium boride composites. *J. Am. Ceram. Soc.*, 1996, **79**(7), 1945–1952.
16. Zhang, G. J. and Jin, Z. Z., Reactive synthesis of AlN/TiB_2 composite. *Ceram. Int.*, 1996, **22**, 143–147.
17. Zhang, G. J., Jin, Z. Z. and Yue, X. M., Reaction synthesis of TiB_2-SiC composites from TiH_2–Si–B_4C. *Mater. Lett.*, 1995, **25**, 97–100.
18. Yoon, S. J. and Jha, A., Vapor-phase reduction and the synthesis of boron-base ceramic phases. *J. Mater. Sci.*, 1995, **30**, 607–614.
19. Weimer, A. W., Moore, W. G., Roach, R. P., Hitt, J. E., Dixit, R. S. and Pratsinis, S. E., Kinetics of carbothermal reduction synthesis of boron carbide. *J. Am. Ceram. Soc.*, 1992, **75**(9), 2509–2514.
20. Chase, M. W. Jr., *NIST-JANAF Thermochemical Tables*, 4th edn. American Chemical Society and the American Institute of Physics for the National Institute of standards and Technology, New York, 1998.
21. Miyata, M. and Yasutomi, Y., Sintering behavior of green compacts of Si and B_4C mixed powder in nitrogen. *J. Ceram. Soc. Japan*, 1994, **102**(10), 936–939.
22. Liu, D. R., Shinozaki, S., Miyata, M. and Yasutomi, Y., Influence of Fe impurity in nitridation of Si + B_4C green compact. *J. Mater. Res.*, 1998, **13**(2), 329–342.
23. Zhang, G. J. and Ohji, T., In situ reaction synthesis of silicon carbide–boron nitride composites. *J. Am. Ceram. Soc.*, 2001, **84**(7), 1475–1479.
24. Zhang, G. J., Beppu, Y., Ohji, T. and Kanzaki, S., Reaction mechanism and microstructure development of strain tolerant in situ SiC–BN composites. *Acta Materiallia*, 2001, **49**(1), 77–82.
25. Zhang, G. J., Yang, J. F. and Ohji, T., Thermogravimetry, differential thermal analysis and mass spectrometry study of the silicon nitride-boron carbide-carbon reaction system for the synthesis of silicon carbide-boron nitride composites. *J. Am. Ceram. Soc.*, 2002, **85**(9), 2256–2260.
26. Zhang, G. J. and Ohji, T., Effect of BN content on elastic modulus and bending strength of SiC–BN in situ composites. *J. Mater. Res.*, 2000, **15**(9), 1876–1880.
27. Zhang, G. J., Yang, J. F., Ando, M. and Ohji, T., Nonoxide–boron nitride composites: in situ synthesis, microstructure and properties. *J. Eur. Ceram. Soc.*, 2002, **22**(14–15), 2551–2554.

28. Munir, Z. A., Synthesis of high temperature materials by self-propagating combustion methods. *Am. Ceram. Soc. Bull.*, 1988, **67**(2), 342–349.
29. Zhang, G. J., Yang, J. F., Deng, Z. Y. and Ohji, T., Effect of Y_2O_3–Al_2O_3 additive on the phase formation and densification process of in situ SiC–BN composite. *J. Ceram. Soc. Jpn.*, 2001, **109**(1), 45–48.
30. Yue, X. M., Zhang, G. J. and Wang, Y. M., Reaction synthesis and mechanical properties of TiB_2–AlN–SiC composites. *J. Eur. Ceram. Soc.*, 1999, **19**(3), 293–298.
31. Massalski, T. B., Okamoto, H., Subramanian, P. R. and Kacprzak, L., *Binary Alloy Phase Diagrams*, 2nd edn. The Materials Information Society, William W. Scott, Jr, USA, 1990, pp. 241–243, 3382–3385.